THE JOURNAL OF COMPARATIVE NEUROLOGY 490:209–219 (2005)

A Compensatory Subpopulation of Motor Neurons in a Mouse Model of Amyotrophic Lateral Sclerosis

ANNELIESE M. SCHAEFER, JOSHUA R. SANES, AND JEFF W. LICHTMAN*
Department of Anatomy and Neurobiology, Washington University School of Medicine, Saint Louis, Missouri 63110

ABSTRACT

Amyotrophic lateral sclerosis is a fatal paralytic disease that targets motor neurons, leading to motor neuron death and widespread denervation atrophy of muscle. Previous electrophysiological data have shown that some motor axon branches attempt to compensate for loss of innervation, resulting in enlarged axonal arbors. Recent histological assays have shown that during the course of the disease some axonal branches die back. We thus asked whether the two types of behavior, die-back and compensatory growth, occur in different branches of single neurons or, alternatively, whether entire motor units are of one type or the other. We used high-resolution in vivo imaging in the G93A SOD1 mouse model, bred to express transgenic yellow fluorescent protein in all or subsets of motor neurons. Time-lapse imaging showed that degenerative axon branches are easily distinguished from those undergoing compensatory reinnervation, showing fragmentation of terminal branches but sparing of the more proximal axon. Reconstruction of entire motor units showed that some were abnormally large. Surprisingly, these large motor units contained few if any degenerating synapses. Some small motor units, however, no longer possessed any neuromuscular contacts at all, giving the appearance of "winter trees." Thus, degenerative versus regenerative changes are largely confined to distinct populations of neurons within the same motor pool. Identification of factors that protect "compensatory" motor neurons from degenerative changes may provide new targets for therapeutic intervention. J. Comp. Neurol. 490: 209–219, 2005.

Indexing terms: sprouting; neuromuscular junction; muscle; reinnervation; motor unit; denervation

Amyotrophic lateral sclerosis (ALS) is a progressive neuromuscular disease in which motor neurons die, leaving muscles denervated. Death from respiratory failure usually occurs within 5 years of diagnosis (Cleveland and Rothstein, 2001). During the past decade, several genes, including SOD1 (Rosen et al., 1993), have been identified that are mutated in heritable cases of ALS, which account for 5–10% of the total (Bruijn et al., 2004). However, no effective treatments are yet available. One factor contributing to this failure may be our ignorance about the sequence of cellular events during disease progression; if we knew more about when and how neuromuscular connections are lost or become reinnervated during the disease process, we would be in a better position to design interventions.

One question in this category is how degenerative and regenerative changes are distributed within diseased muscles. In patients and in animal models, loss of neuromuscular junctions leaves muscle fibers denervated. Intact axonal branches then sprout to sites in a compensatory process that prolongs motor function transiently but eventually fails to keep pace with the accelerating rate of

Grant sponsor: National Institutes of Health; Grant number: NS020364; Grant number: NS034448 (to J.W.L., J.R.S.); Grant sponsor: Project A.L.S. (to J.W.L., J.R.S.); Grant sponsor: Helen Hay Whitney Postdoctoral Fellowship (to A.M.S.).

Dr. Sanes's and Dr. Lichtman's current address is Department of Molecular and Cellular Biology, Harvard University, Cambridge, MA 02138.

*Correspondence to: Jeff Lichtman, Department of Molecular and Cellular Biology, Harvard University, Cambridge, MA 02138.
E-mail: jeff@mcb.harvard.edu

Received 19 November 2004; Revised 18 February 2005; Accepted 22 March 2005

DOI 10.1002/cne.20620

Published online in Wiley InterScience (www.interscience.wiley.com).

denervation (Buchthal and Pinelli, 1953; Wohlfart, 1957, 1958; Gurney et al., 1994). Recently, Fischer et al. (2004) and we (Schaefer et al., 2002) noted that, in a mouse model of this disease, axon pathology appeared to be dying back, with intact proximal axons and absent neuromuscular junctions. This histopathology raised the possibility that some axonal branches are spared during the disease whereas others degenerate. We sought to understand how loss and growth occur at individual neuromuscular junctions and whether such opposing events can occur in different branches of the same neuron or, alternatively, whether whole motor units are either compensating or degenerative.

Evidence from developmental axon branch removal shows that individual motor neurons simultaneously withdraw some branches while enlarging others to expand their synaptic connections (Keller-Peck et al., 2001; Walsh and Lichtman, 2003). It is also possible, however, that some subset of motor neurons is particularly susceptible to the disease whereas another group is more refractory and thus able to compensate for a time. If this were the case, understanding what makes some neurons more refractory than others might provide a useful starting point for designing therapeutic interventions.

Here we have attempted to distinguish between these alternatives in a mouse model of ALS. Transgenic mice expressing any of several mutant human SOD1 alleles (but not mice overexpressing wild-type SOD1 or mice lacking endogenous SOD1) show many features of the human disease, including adult-onset muscle weakness, motor neuron loss, and premature death (Gurney et al., 1994; Ripps et al., 1995; Wong et al., 1995; Reaume et al., 1996; Bruijn et al., 1997, 2004). Of these transgenic lines, we used the one (G93A; Gurney et al., 1994) that has been studied most intensively. First, we bred G93A SOD1 animals to transgenic mice in which all motor axons are indelibly marked by the yellow fluorescent protein (YFP; Feng et al., 2000). High-resolution confocal imaging of neuromuscular junctions and axons in SOD1 animals revealed several distinct appearances, including axonal branches that appeared to be normal except that they were fragmented at their contact sites with muscle fibers.

Time-lapse imaging of nerve terminals in these mice in vivo showed us that such fragmented terminal axons were in the process of disconnecting from muscle fibers and could be distinguished from axon branches that were in the process of reinnervating neuromuscular junctions. Then we examined G93A SOD1/YFP double transgenics in which only one or a few motor axons were labeled within each muscle (Feng et al., 2000; Keller-Peck et al., 2001; Nguyen et al., 2002). Reconstruction of entire motor units in these mice revealed two kinds of arbors: some that largely or exclusively contained branches that were fragmented and disconnected from neuromuscular junctions, and others that contained normal or thin reinnervating branches. We conclude that two types of motor neurons within individual motor pools, "losers" and "compensators," play fundamentally different roles in ALS.

MATERIALS AND METHODS

Mice

Transgenic *thy1*-YFP-H and *thy1*-YFP-16 mice were generated as described previously (Feng et al., 2000) and maintained in a C57Bl6 background. All analyses were done by using the G93A SOD1 G1H strain (Chiu et al., 1995). G93A SOD1 mice were bred to *thy1*-YFP animals; G93A SOD1 progeny were indistinguishable from G93A SOD1/YFP littermates in terms of disease onset and progression. In this study, *presymptomatic* animals (indistinguishable from wild-type littermates) were postnatal day (P)41–77; *symptomatic* (hindlimbs trembled and pulled in on raising the tail) were P81–119; and *end stage* (hindlimb paralysis) were P123–145. YFP transgenics and transgenic G93A SOD1 animals are available from Jackson Laboratories (Bar Harbor, ME).

All analyses conformed to NIH guidelines and were carried out under an animal protocol approved by the Washington University Animal Studies Committee.

Tissue staining

Mice were deeply anesthetized with sodium pentobarbital and perfused transcardially with 2% paraformaldehyde in 0.1 M phosphate-buffered saline (PBS; pH 7.4). Muscles dissected included the sternomastoid, cleidomastoid, and clavotrapezius in the neck, the diaphragm, and the extensor digitorum longus (edl) and soleus in the hindlimb. Tissue was postfixed in paraformaldehyde for 1 hour, the connective tissue was removed, and muscles were incubated for 30 minutes at room temperature in 5 μg/ml Alexa 594- or Alexa 647-conjugated α-bungarotoxin (Molecular Probes, Eugene, OR) diluted in 1% bovine serum albumin (BSA) in sterile lactated Ringer's solution. Muscles to be immunostained were blocked in 4% BSA and 0.4% Triton-X in PBS overnight at 4°C.

The following day, tissue was incubated in primary antibody for 1–3 days. Primary antibodies used were anti-green fluorescent protein (GFP) rabbit polyclonal made against highly purified native GFP from *Aequorea victoria* (1:400; lot number 23100825; Chemicon, Temecula, CA), neurofilament 150 polyclonal made against highly purified bovine neurofilament-M polypeptide (1:100; lot number 231018UO; Chemicon), and S100 rabbit polyclonal made against S100 isolated from bovine brain (1:100; lot number 019H4809; Dako, Glostrup, Denmark). After washing for 5 hours in PBS, muscles were incubated in secondary antibody overnight at 4°C. Secondary antibodies used were Alexa 488 anti-rabbit (Molecular Probes) 1:500 and rhodamine anti-rabbit (Cappel, Aurora, OH) 1:400. After washing for 5 hours in PBS, muscles were whole-mounted on slides in Vectashield (Vector, Burlingame, CA). For controls, the primary antibody incubation step was omitted from the protocol. Additionally, for the anti-GFP antibody, staining is absent in animals that do not transgenically express fluorescent protein. For the neurofilament 150 antibody, see also Hafezparast et al. (2003) and Ohshima et al. (2002). For the S100 antibody, see also Love and Thompson (1998).

Imaging and analysis

Motor units and neuromuscular junctions were imaged on a laser scanning confocal microscope (Olympus FV500, Melville, NY; or Bio-Rad 1024, Hercules, CA with an Olympus BX50WI microscope). Images were obtained by using 25× Zeiss Plan Neofluor multi-immersion (0.8 NA) or Olympus Plan Apo 60× oil (1.4 NA) objectives. Z stacks were flattened with Confocal Assistant. Some motor units were scored by using epifluorescence and 25× (0.6 NA) and 50× (1.0 NA) water objectives.

Motor unit analyses

Muscles dissected for motor unit analyses were the sternomastoid, clavotrapezius, and cleidomastoid. Some muscles were immunostained with anti-GFP antibody (Chemicon) to enhance the YFP signal. We used Monte Carlo analysis to determine the likelihood that fragmented axons were randomly distributed across all motor units, given the number and size of motor units. Code was written by T. Holy for MATLAB software and tested by using 10,000 synthetic datasets. Results were compared against randomly generated datasets that maintained the total number of motor units and their size but shuffled and redistributed the junctions. This process was repeated to test the likelihood that the thin axons were randomly distributed across motor units. In both cases, the *P* value approached 0 (one-sided test).

In vivo time-lapse imaging

Mice were anesthetized with a subcutaneous injection of KX in sterile saline (ketamine at 887 mg per kg body weight; and xylazine at 13 mg per kg body weight). A superficial incision was made in the ventral neck, and approximately 2% of the acetylcholine receptors (AChRs) in the sternomastoid muscle were labeled with Alexa 594-conjugated α-bungarotoxin (Molecular Probes). Superficial junctions were imaged at 25× (water immersion objective, 0.6 NA) and 50× (water immersion objective, 1.0 NA) by using standard epifluorescence microscopy and a QImaging Retiga EXi cooled CCD camera. The wound was then sutured, and the animal was placed in a heated, oxygenated chamber until it was sufficiently recovered and active to be returned to its cage. This procedure was repeated for subsequent imaging sessions.

RESULTS

Denervating and reinnervating neuromuscular junctions in SOD1 transgenic mice

We imaged neuromuscular junctions in double transgenic mice that ubiquitously expressed mutant SOD1 (Gurney et al., 1994; Chiu et al., 1995) and expressed YFP in all motor neurons (Feng et al., 2000). We first studied animals at P125–P144. These animals were near the end stage of the disease and had complete hindlimb paralysis. Junctions were studied by confocal imaging of axon arbors and postsynaptic acetylcholine receptors (AChRs; see Materials and Methods). Muscles examined included the sternomastoid and clavotrapezius of the neck, the edl and soleus of the hindlimb, and the diaphragm. In these animals, some junctions (ranging from 6% in the edl [n = 174] to 48% in clavotrapezius [n = 291]) were indistinguishable from those in age-matched controls (compare Fig. 1A, junction A3 and Fig. 1C1 with junction in Fig.1B): the axon entering each neuromuscular junction was thick and variegated in diameter, terminal branches were uniform in width, and AChR-rich sites on each muscle fiber were closely apposed to terminal branches. However, other junctions were abnormal. These junctions fell into several categories, as described below.

At some junctions the postsynaptic apparatus was completely denervated. Postsynaptic specializations at the majority of these denervated sites (two-thirds, or 207/308 in the sternomastoid) looked like those in controls (Fig. 1C2); at the rest, postsynaptic sites were AChR-poor and disorganized in shape (Fig. 1C3), suggesting that they had been denervated for several weeks (Frank et al., 1975; Rich and Lichtman, 1989).

At another set of junctions, postsynaptic sites were partially occupied by nerve terminals. These partially innervated junctions could be further subdivided. In some, the axon appeared fragmented at its terminal with remnants of YFP overlying the junction (Fig. 1C4) or in close proximity (Fig. 1C5). At other junctions, the axon was continuous rather than fragmented but abnormally thin and smooth. Such branches were most frequently seen in apposition to normal-looking receptor sites (Fig. 1C6), but at some junctions, the thin branches apposed faint receptor sites (Fig. 1C7).

These different morphologies were similarly distributed in five different muscles (Fig. 1D). Moreover, we confirmed that YFP was a representative marker of axonal morphology, by immunostaining for neurofilament (Fig. 2).

We were interested in understanding the relationship between these phenotypes and the stages of the disease. As a first step, we noted that two of the phenotypes might signify the point of axon removal: fragmented axon tips resembled fragmentation seen in Wallerian degeneration after axotomy, whereas thin smooth branches resembled those undergoing removal during naturally occurring synapse elimination (Keller-Peck et al., 2001). We therefore imaged individual neuromuscular junctions in the sternomastoid muscle at multiple time points (see Materials and Methods) to obtain a cellular description of the pathological course of the disease.

In wild-type animals, junctions are very stable, showing few alterations in presynaptic terminal branch morphology or postsynaptic receptor appearance over long periods (Balice-Gordon and Lichtman, 1990). Similarly, none of the junctions imaged in presymptomatic G93A SOD1 animals (n = 29 at P41–77) changed significantly during the 3–28-day intervals between views (Fig. 3A). In symptomatic and end-stage animals, however, 21 of the 71 junctions imaged underwent significant changes over time. For example, in one muscle we observed adjacent muscle fibers undergoing opposite changes over 10 days. In particular, a motor axon terminating in a normal-looking neuromuscular junction became fragmented at a second view, whereas a denervated junction with nearby fragments was reinnervated by a thin smooth axon (Fig. 3B). These observations show that the opposing processes of loss and growth have distinct morphological signatures.

The following discussion summarizes all alterations observed from the time-lapse images: normal morphology to fragmented (n = 2); normal to denervated (n = 4); fragmented to thin smooth axon (n = 1); normal to thin smooth axon (n = 8); thin smooth axon became more irregular in caliber (n = 3); and thin smooth axon increased occupancy of the site (n = 3). Importantly, of the 15 neuromuscular junctions with thin smooth axons at the first view, none were fragmented or absent at the second view: 9 remained unchanged whereas the other 6, as noted above, expanded.

We draw three conclusions from these results. First, the lack of degenerative changes of thin smooth axons suggests that these inputs are in the process of reinnervating rather than being lost. Second, as expected, junctions occupied by fragmented axons are in the process of being denervated. Third, the low incidence of fragmented axons

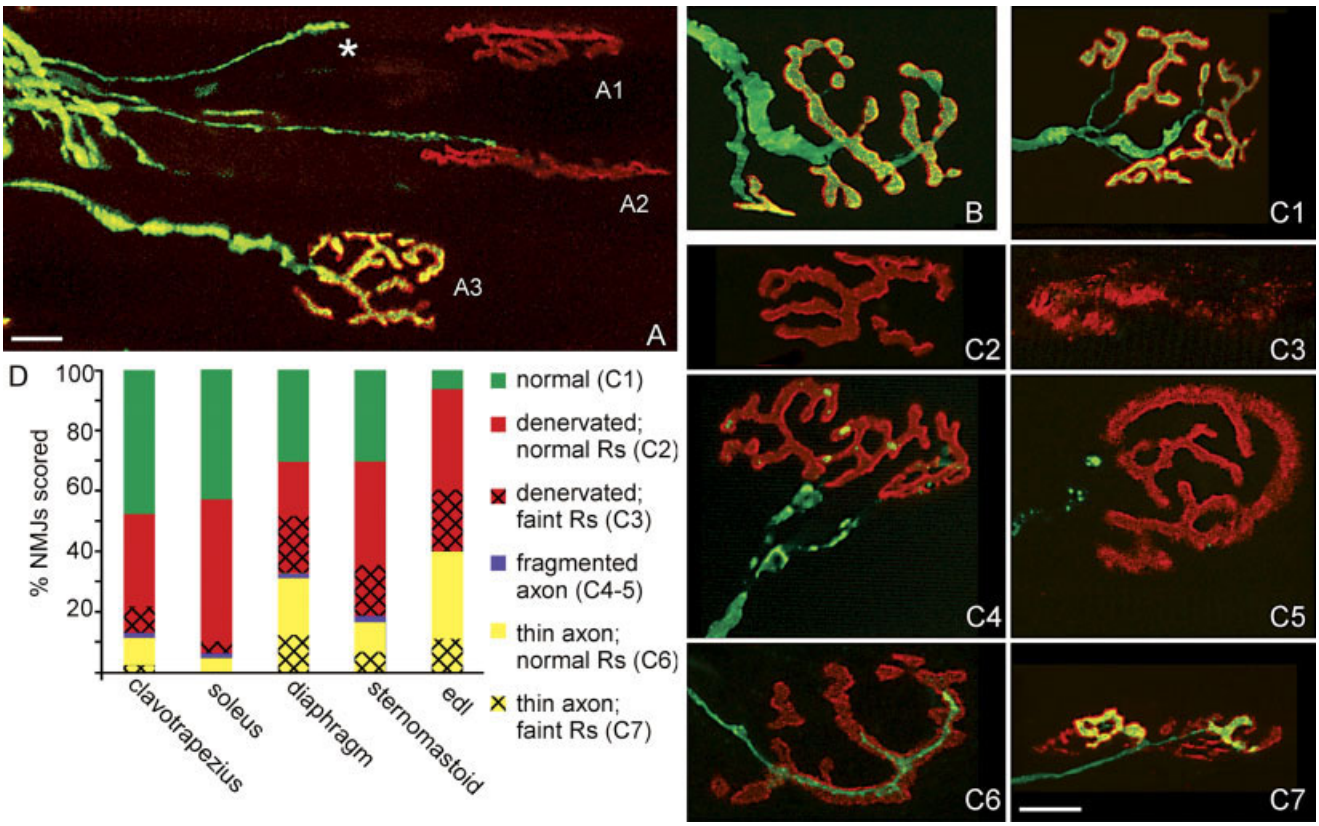

Fig. 1. Diverse morphologies at neuromuscular junctions in G93A SOD1/YFP16 muscle. **A:** Neuromuscular junctions (NMJs) on adjacent muscle fibers in SOD1 end-stage mice show a range of abnormalities, as revealed by the cytoplasmic YFP (green) labeling in the presynaptic axons and Alexa 594-tagged α-bungarotoxin (red) bound to the postsynaptic AChRs. Whereas some junctions appear to be normal (**A3**), others are completely denervated with normal AChR morphology (**A1**). Sometimes, however, the AChRs are also abnormal, appearing disorganized and faint (**A2**). The thin axon near junction A1 (asterisk) and another contacting junction A2 probably represent reinnervating axons (see Results). **B:** A neuromuscular junction from a control adult animal showing characteristic features, including a thick but variegated distal axon and terminal branches that are uniform and closely apposed to AChRs. **C:** Categories of terminal axon morphologies in G93A SOD1 mice. Some junctions appear normal (**C1**). Others have normal AChRs but completely lack presynaptic axons (**C2**). Occasionally, unapposed AChRs look faint and disorganized (**C3**). Some junctions contain fragments of YFP apposed to receptors with normal morphology (**C4**). Slightly proximal to the junction, the presynaptic axon appears normal. Occasionally, the axon is fragmented but no longer apposes the junction (**C5**). Terminal branches sometimes are thin and smooth and only partially occupy the AChR site (C6,7). Junctions contacted by thin axons have either normal AChR morphology (**C6**) or AChRs that are faint and appear disorganized (**C7**). **D:** Muscles from end-stage G93A SOD1 mice show different degrees of disease but have a similar distribution of junctional phenotypes ($P < 0.0001$, Chi-squared test for independence). edl, extensor digitorum longus muscle; Rs, receptors. (The neuromuscular junctions in A,B,C5,C6 are from the sternomastoid muscle; the junctions in C1–C4 and C7 are from the clavotrapezius muscle.) Scale bar = 20 μm in A; 20 μm in C7 (applies to B–C7).

suggests that the process of denervation occurs rapidly. This rapidity may account for the junctions that were normal at the first view but were occupied by a thin axon at the second: they had undergone denervation and reinnervation during the 5–14-day interval between views.

Comparison of single-time-point images in the sternomastoid muscle of presymptomatic, symptomatic, or end-stage animals (Table 1) was compatible with the scheme derived from time-lapse data. First, there were few fragmented distal axons at any of these stages, supporting the idea that this step is rapid. Second, the number of thin and smooth terminal axon branches increased as the disease progressed; these axon branches may represent compensatory synaptogenesis at sites where axons had previously fragmented. Third, the number of denervated junctions increased dramatically with age, reaching 51.2% in end-stage animals. One-third of these (16.8/51.2) had faintly labeled AChRs, suggesting that compensatory axon growth mechanisms could not keep pace with the rate of denervation.

Two observations suggest that presynaptic axons degenerate prior to degenerative changes in either the muscle fiber or Schwann (glial) cell. First, although the presynaptic nerve terminal was often abnormal when the postsynaptic structure looked normal, we never observed dim or otherwise abnormal AChRs innervated by a normal axon. Second, there was no significant difference in the number of terminal Schwann cell nuclei at neuromuscular junctions in end-stage G93A SOD1 mice versus age-matched controls, as shown by immunostaining for S100 (G93A SOD1: 2.54 ± 1.21 nuclei/junction; controls: 2.89 ± 1.16 Schwann cell nuclei/junction; Mann-Whitney nonparametric test). These results suggest that the earliest changes in the disease are found at the terminal branches

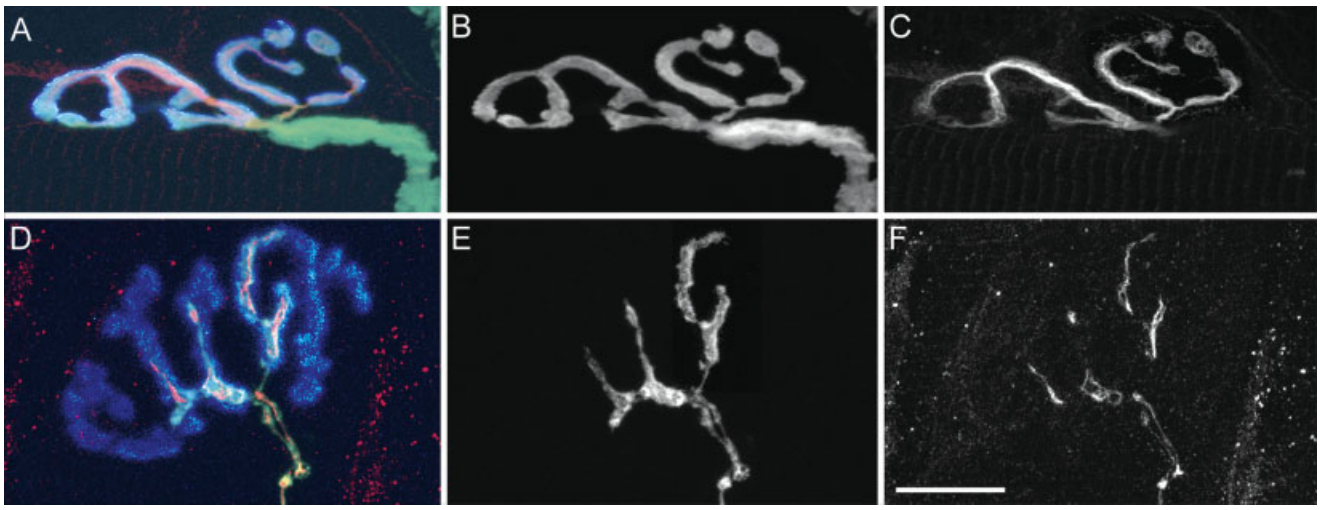

Fig. 2. YFP is a representative marker of axonal morphology. In the sternomastoid muscle of a control animal (**A**), terminal axon branches labeled by YFP (green) and neurofilament immunostaining (red) are closely apposed to AChRs labeled by α-bungarotoxin (blue). Single-channel images in grayscale show the overlapping patterns of terminal branch morphology revealed by YFP (**B**) or neurofilament staining (**C**). In G93A SOD1 mice, terminal axon branches often fail to cover AChRs (**D**). Single-channel images show that the branch morphology revealed by YFP expression (**E**) closely matches that shown by neurofilament staining (**F**). Scale bar = 20 μm in F (applies to A–F).

of motor axons and invoke a model whereby neuromuscular junctions proceed through a stereotypic series of steps in the course of denervation and reinnervation (Fig. 4).

Distribution of fragmenting and re-growing terminal branches within motor units

How are branch loss and growth apportioned within single motor units? At one extreme, each motor axon could contain a mixture of dying and growing junctions in proportion to their incidence in the whole muscle. At the other extreme, some motor axons might withdraw from most or all of the junctions they initially innervate, whereas others predominantly sprout to occupy denervated sites. To distinguish between these and other alternatives, we bred G93A SOD1 transgenic mice to transgenic animals expressing YFP in a small subset of motor neurons (Feng et al., 2000) and then reconstructed entire motor units (Keller-Peck et al., 2001; Kasthuri and Lichtman, 2003). YFP-H marks an apparently random subset of motor neurons that includes those innervating both fast-twitch and slow-twitch muscle fibers (S. Kuang, M. Buffelli, L. Baylor, J.W.L., and J.R.S., unpublished observations). Each junction was assigned to one of the categories described above (Fig. 1). Examples are shown in Figure 5, and all data are summarized in Figure 6.

In wild-type control motor units, every terminal branch contacted and completely occupied a receptor-rich postsynaptic apparatus (data not shown; see Nguyen et al., 2002). Motor units in G93A SOD1 mice fell into three distinct categories. One class was essentially normal (motor units #4, #6, and #12 in Fig. 6A) and may represent motor neurons not yet obviously affected by the disease. A second class contained fragmented axonal branches but no reinnervating (thin smooth) branches (Fig. 5A,B; motor units #3, #9, #11, and #14 in Fig. 6A). Two of these motor units (#3 and #11) retained some normal junctions, indicating that denervation occurs at different rates on different muscle fibers (see also Fig. 5A). Two other units (#9 and #14) were comprised solely of fragmented branches. Interestingly, the parent axon and proximal branching of these motor units appeared normal, giving them a "winter tree" appearance (Fig. 5B). These data indicate that the earliest morphological changes are at the most distal parts of the axon branches (Fischer et al., 2004). We also observed axons that no longer contained any terminal branches and were fragmented more proximally (n = 19). These axons could not be traced to any junctions. Such severely degenerated axons may reflect winter tree motor units in yet a more advanced stage: they have lost not only "leaves" but also "branches."

Junctions in the third class of motor units contained reinnervating (thin smooth) branches but few or no fragmented branches (Figs. 5C, 6A: motor units #1, #2, #5, #7, #8, #10, #13, and #15–26). Only three motor units in this class contained any fragmented branches; these were $<3\%$ of the junctions in each motor unit (Fig. 6A: 1/37 in #16; 2/72 in #21; and 2/100 in #22) and $<1\%$ of the junctions in the category as a whole. Moreover, most of the motor units in this category (13/19) were larger than any seen in wild-type muscles. We rarely saw terminal sprouting in these muscles, indicating that the growth was probably initiated by sprouts at nodes of Ranvier (Chiu et al., 1995). We surmise that these motor units underwent massive sprouting to occupy junctions vacated by winter tree motor units. Additionally, the number of *normal-looking* junctions in these motor units was sometimes greater than the *total* number of junctions in wild-type motor units (for example, 63, 44, and 127 normal junctions in motor units #23, #24, and #26, respectively, compared with a maximum of 27 junctions among the seven wild-type motor units; Fig. 6A). This comparison suggests that some reinnervating axon branches eventually matured to acquire a normal adult appearance.

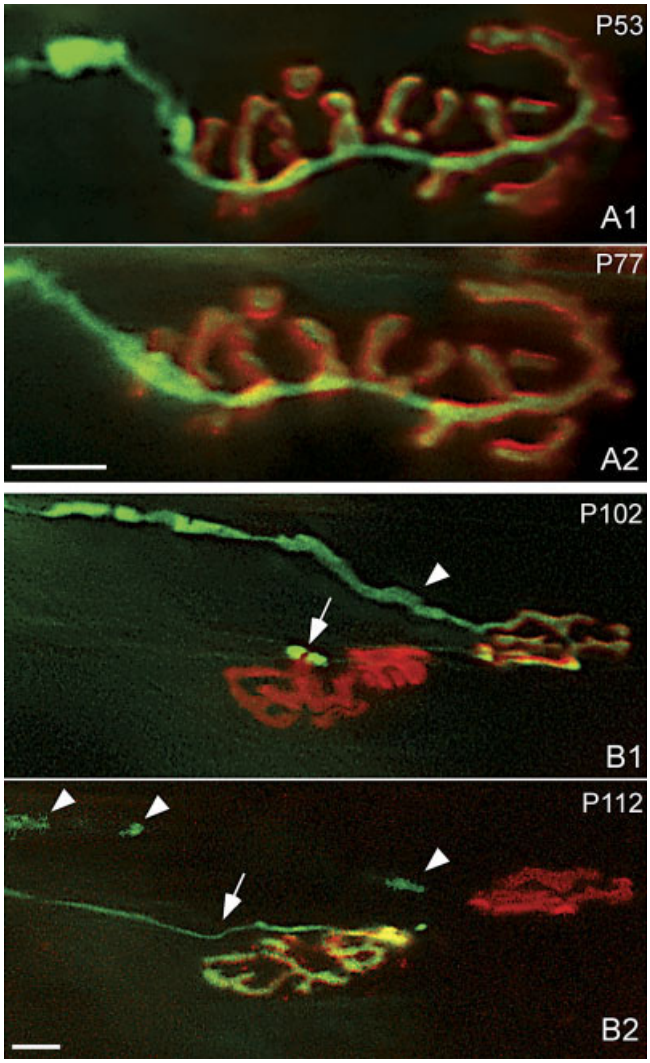

Fig. 3. In vivo time-lapse imaging of neuromuscular junctions in G93A SOD1 mice. **A:** Synapses in the sternomastoid muscle of young asymptomatic G93A SOD1 mice are normal and stable over weeks. There is no significant change in the mature pretzel pattern of this junction from the first view at P53 (**A1**) to the second view 3½ weeks later at P77 (**A2**). (Green: YFP-labeled axon; red: Alexa 594 α-bungarotoxin to label AChRs on muscle fiber.) **B:** In symptomatic animals, we directly observed synapses become denervated and reinnervated. A normal junction with a thick axon (**B1**, arrowhead) at P102 becomes denervated by P112, and its axon has become fragmented (**B2**, arrowheads). An adjacent denervated junction shows only fragments of YFP at the first view (B1, arrow) but, at the second view, is reinnervated by a thin smooth axon (B2, arrow). Scale bar = 20 μm in A2 (applies to A1,A2); 20 μm in B2 (applies to B1,B2).

To ask whether this apparently bimodal distribution of motor units was statistically significant, we performed a Monte Carlo analysis. This analysis demonstrated that the distribution of the fragmented as well as the thin terminal branches was highly skewed ($P < 10^{-13}$ for each that this was a chance occurrence, one-sided test; see Materials and Methods).

Finally, because the number of whole motor units available for analysis was limited, we also analyzed parts of motor units. We identified 20 sets of 3–12 junctions that could be assigned to a single motor unit, even though the entire motor unit could not be traced because it was deep within a muscle or intermingled with branches of another labeled axon (see, for example, Fig. 5A). Of these 20 sets, 8 showed the fragmented phenotype, 12 contained thin axons, and none contained both fragmented and thin axons (Fig. 6B). These data support the conclusion that individual motor neurons projecting to a single muscle in ALS model mice are in the process of degenerating or compensating but not both (Fig. 7).

DISCUSSION

Our main conclusion is that, in a genetically valid mouse model of ALS, individual motor pools contain two distinct types of motor neurons, "losers" (which contain fragmented, degenerating branches) and "compensators" (which contain thin, reinnervating branches). Several results support this conclusion. First, the distribution of degenerating terminal branches among complete motor units was highly skewed ($P < 10^{-13}$), as was the distribution of thin branches ($P < 10^{-13}$). Second, motor units containing newly elaborated branches seldom (3/19 motor units) had degenerating axon branches. In these three examples, degenerating branches comprised a very small fraction (2–3%) of the total motor unit. Third, this same bimodality was observed in partial motor units: individual neurons contained degenerating or growing axons, but never both. Fourth, motor axons containing new growth frequently (13/19) contacted more muscle fibers than wild-type motor axons, evidence of their ability to compensate for the loss of other axons.

That a subset of neurons within a motor neuron pool is refractory is a novel finding. It has been suggested that, in ALS, small-caliber axons persist (Kawamura et al., 1981; Bruijn et al., 1997, 2004). In cross sections of ventral roots in the lumbar spinal cord of ALS patients as well as in the G85R SOD1 transgenic mouse model of ALS, the number of large-caliber axons is significantly lower than in controls, but the number of small-caliber axons is maintained (Dyck et al., 1975; Bradley et al., 1983). However, thin axons may represent new growth rather than persistent axons. Our results show that new growth occurs in the form of thin branches and that these thin branches emanate primarily from axons, as opposed to terminal sprouts

TABLE 1. Percent Distributions of Synaptic Phenotypes in the Sternomastoid During Disease Progression

		Denervated			Thin axon		
	Normal	normal Rs	faint Rs	Fragmented axon	Normal Rs	Faint Rs	No. of (junctions scored)
Presymptomatic	97.8	0	0	1.6	0.6	0	314
Symptomatic	92.6	0.9	1.6	0	4.4	0.5	435
End stage	30.3	34.4	16.8	2.2	9.9	6.5	601

Rs, receptors.

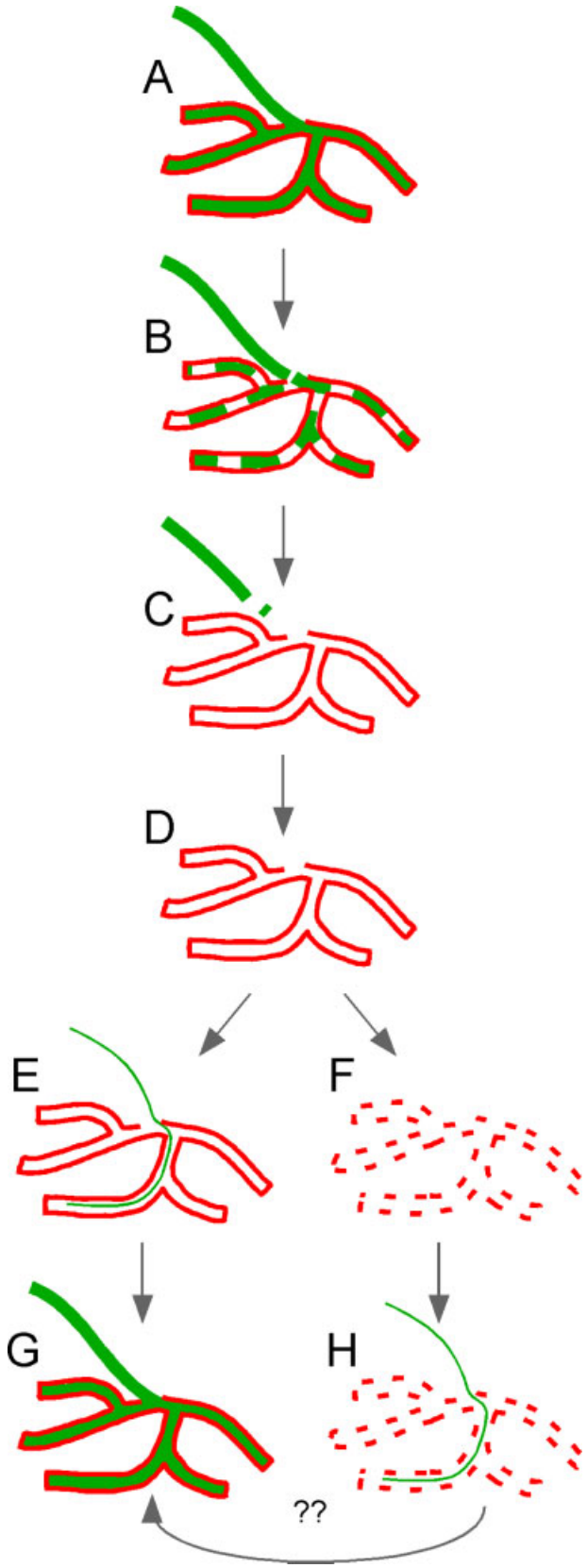

(see also Chiu et al., 1995). Thus, single-time-point observations of ventral roots cannot distinguish thin axons that persisted from new thin axons that are compensatory.

These results would have been difficult to obtain without the use of YFP transgenic mice, which made it possible to visualize fine detail at neuromuscular junctions, to image individual synapses at multiple time points and to reconstruct individual motor units. However, our conclusions are consistent with several previous findings. First, electromyographic and histochemical studies indicate that motor axons in ALS patients expand during the course of disease (McComas et al., 1971; Dengler et al., 1990; Brown and Chang, 2000). Indeed, enlarged motor unit potentials, which indicate compensatory reinnervation, are used clinically in differentiating ALS from myopathic diseases (Brown, 2004). As predicted from such previous data, we observed motor units in the G93A SOD1 mouse model that were much bigger than in control animals. We were surprised, however, that such motor units appeared robust and markedly distinct from winter tree motor units.

Second, Fischer et al. (2004) used immunocytochemistry on cryosections to show that neuropathological changes in ALS model mice occur earlier in muscle than in ventral root or spinal cord. That work described "intermediate" neuromuscular junctions, in which axonal branches incompletely apposed AChRs. Our observations resolve the status of "intermediate" junctions as being in the process of either denervation or reinnervation and show that junctions in the process of denervation have a unique appearance of fragmentation. This finding, in turn, enabled us to distinguish patterns in individual motor units and to identify a subgroup of refractory motor axons.

Third, there is precedent for sparing of certain muscles in ALS: the muscles that control eye movements and bladder function are relatively unaffected, suggesting that the motor neurons innervating them (in oculomotor nuclei and Onuf's nucleus, respectively) are relatively resistant to neurodegeneration. These data have led to a search for special properties of the target muscles innervated by these motor pools. By showing that such sparing also occurs within a single motor pool, our results motivate a search for intrinsic distinctions among motoneurons.

Fourth, Frey et al. (2000) have shown that, in G93A SOD1 mice, regions of the triceps surae muscles relatively rich in slow-twitch fibers show denervation at later stages than regions relatively rich in fast-twitch fibers. They interpreted their results as indicating that slow motor neurons are more resistant than fast motor neurons to the effects of toxic SOD1. Although their results are consis-

Fig. 4. Model for changes at a single neuromuscular junction during disease progression in ALS. **A:** Neuromuscular junctions in normal animals and in young G93A SOD mice have uniformly sized terminal axonal branches (green) that are closely apposed to AChRs (red). **B:** In these mice, terminal axon branches fragment, but the proximal axon retains a normal appearance and the postsynaptic AChR morphology is unchanged. **C:** Eventually, the neuromuscular junction becomes completely denervated, but the receptors maintain normal morphology (**D**). Some denervated junctions become partially reinnervated by a thin growing axon (**E**); some of these axons probably mature into normal-appearing nerve terminals (**G**). At neuromuscular junctions that remain denervated, AChRs become faint and disorganized (**F**), although some of these AChRs become apposed by new axon branches (**H**).

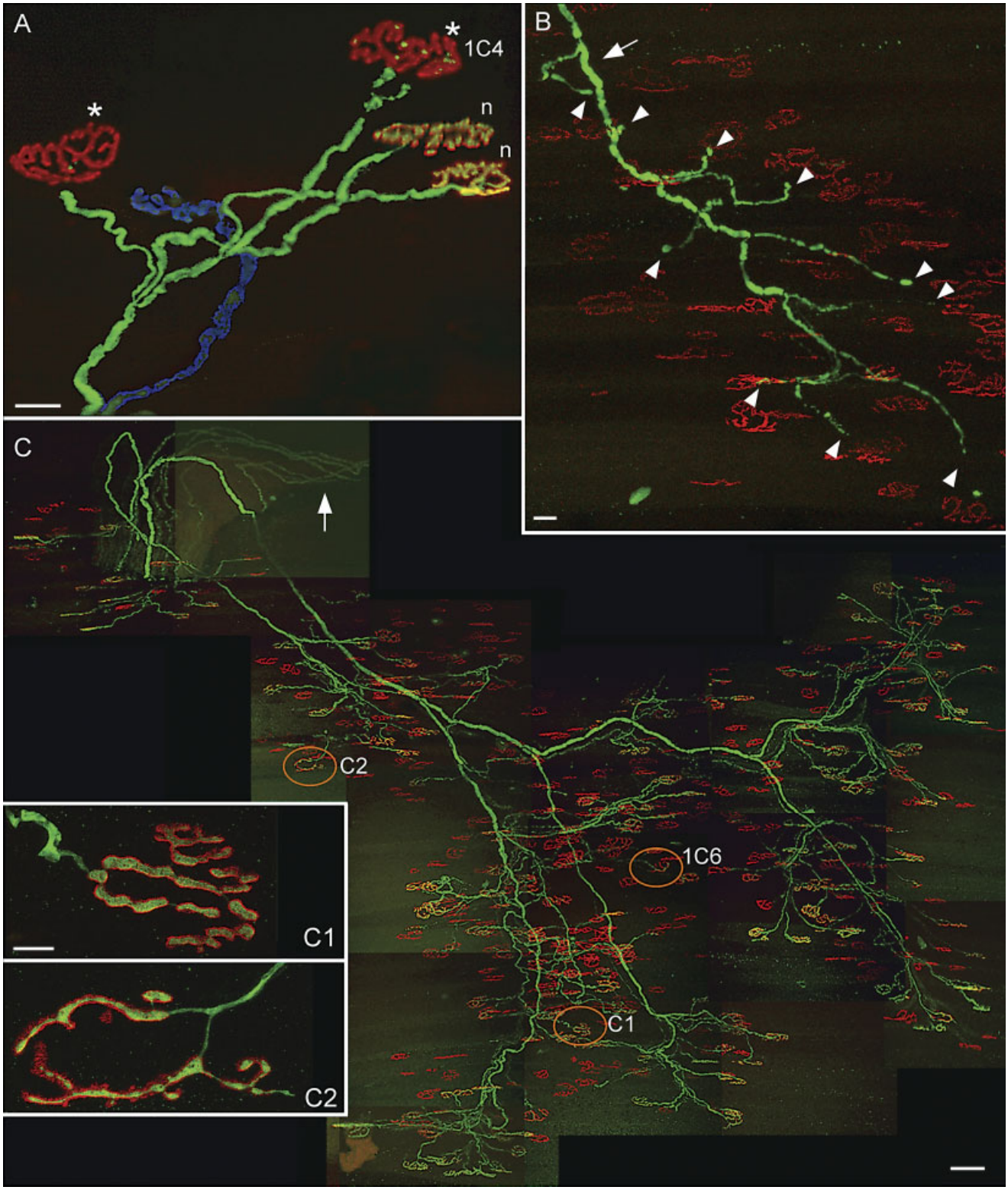

Fig. 5. Motor units show fragmentation or growth in G93A SOD1 mice. **A:** Fragmented terminal axon branches are intermixed with normal-appearing terminal branches in some motor units. Shown is a confocal reconstruction of an axon's projection to four nearby neuromuscular junctions in the clavotrapezius muscle of a symptomatic animal. Two of the junctions innervated by this axon are normal (n), but at two others only fragments of YFP from the presynaptic axon remain (asterisks). One fragmented junction is shown at higher magnification in Figure 1C4. This variety of branch morphologies within a single motor unit indicates that neuromuscular abnormalities occur asynchronously among different branches of the same axon. Interestingly, the slightly more proximal parts of each terminal branch are all indistinguishable, suggesting that the abnormality is initially confined to the most distal parts of branches. An axon from a separate motor unit has been rendered blue by using Adobe Photoshop. **B:** A complete motor unit in the sternomastoid muscle that lacks a single normal junction (#14 in Fig. 6A). All the distal axons terminate in a blunt or fragmented way (arrowheads). Despite the terminal abnormalities, the more proximal axon branches appear normal (arrow), containing nodes of Ranvier and a variegated appearance, giving the entire motor unit the look of a winter tree. **C:** In contrast to winter tree motor units, some motor units contain normal as well as newly growing branches. The motor unit shown here (#26 in Fig. 6A) from a sternomastoid muscle contacts 175 muscle fibers, making it substantially larger than the normal motor unit size. Junctions are normal (see inset, **C1**) or contain thin axons (see inset, **C2** and Fig. 1C6). Additional YFP-labeled axons (arrow) project to a different region of the muscle. Scale bar = 25 μm in A; 25 μm in B; 100 μm in C; 10 μm in C1 (applies to C1,C2).

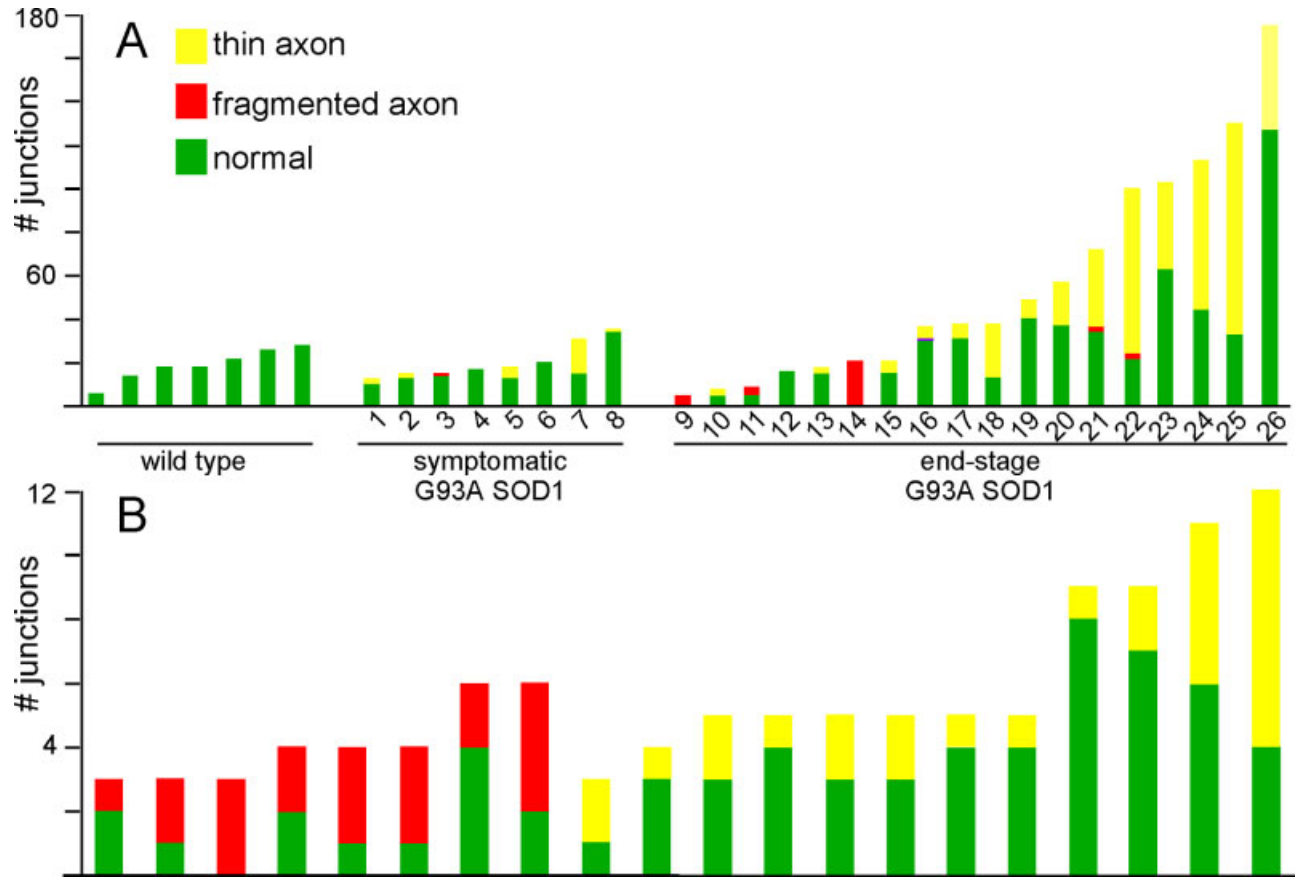

Fig. 6. Motor unit composition reveals two populations of motor neurons. **A:** Neuromuscular junctions within single motor units of the sternomastoid, clavotrapezius, and cleidomastoid muscles are categorized as normal (green), reinnervated (supplied by a thin smooth axon, light green), or denervating (near a fragmented axon, red). Each motor unit (bar) from wild-type animals contains normal neuromuscular junctions and ranges in size from 6 to 27 neuromuscular junctions. In G93A SOD1 mice, most motor units contain either fragmented or thin axons but rarely both. The distribution of these phenotypes is highly skewed among motor units ($P < 10^{-13}$, Monte Carlo analyses; see Materials and Methods). **B:** Partial motor units (junctions that could be assigned to a single motor axon even when entire motor units could not be traced) show the same bimodal distribution as complete motor units: they contain normal neuromuscular junctions plus either fragmented axons or thin axons but not both.

tent with the idea that motor neurons within a pool differ in their susceptibility to the disease, the distinction between slow- and fast-twitch fibers cannot explain the bimodal neuronal responses reported here, because the muscles we studied have few slow fibers. Moreover, we are suggesting that certain motor neurons are refractory to degeneration, as opposed to degenerating on a slower time scale.

We conclude that there are distinct subpopulations of motor neurons because winter tree motor units were not enlarged and showed no signs of growth, whereas compensators showed little to no sign of loss. We do not know, however, whether there are only two divisions with respect to vigor, or multiple classes. We also do not know whether compensators are absolutely refractory to disease, or whether they are relatively refractory and would eventually be stricken. Such questions might be addressed in a preliminary way by analyzing motor units in muscles that are affected earlier or later in the disease (Fig. 1D). Definitive answers may not be obtained until molecular correlates of the alternative fates are discovered.

What could account for the differences in susceptibility among motor units? We imagine four classes of mechanisms. The first is stochastic: essential random fluctuations in some quality may reach a threshold value that starts some motor neurons on an irreversible path to their demise. Such stochastic mechanisms have been invoked in cell fate choices during development and aging (Herndon et al., 2002) and could also help explain the course of slowly progressive diseases such as ALS. A second is that the relevant variation is external to the motor neuron itself. Recent studies of chimeric mice have shown that some effects of SOD1 on motor neuron survival are non-cell-autonomous (Clement et al., 2003); perhaps losers and compensators are subject to different influences from neighboring interneurons, astrocytes, or microglia (Clement et al., 2003), from the vasculature (Oosthuyse et al., 2001; Azzouz et al., 2004), or from the muscle fibers they innervate. Third, and most simply, motor neurons might vary in the level of SOD1 they express.

The fourth and most interesting class of mechanism is one in which motor neurons differ in some endogenous

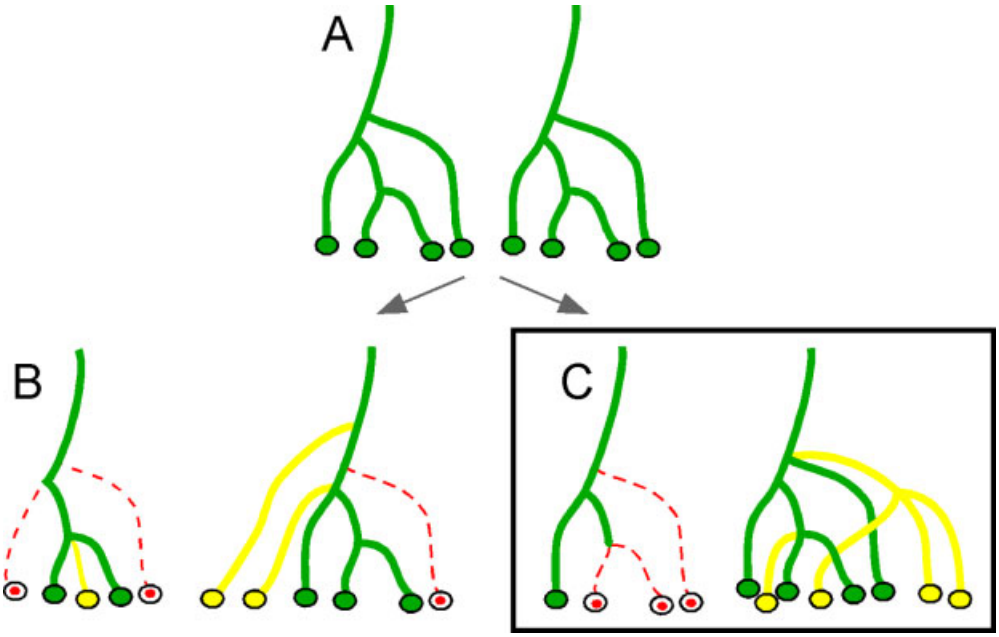

Fig. 7. Alternative models for changes in individual motor units during disease progression in the G93A SOD1 mouse model of ALS. **A:** Motor units initially contain uniformly-sized axons and normal neuromuscular junctions (black circles). In one alternative (**B**), each motor unit shows loss and growth, containing a mixture of denervating (red) and reinnervating (light green) terminal axons. In a second alternative (**C**) supported by our results, some motor units remove their synaptic terminals from muscle fibers, while others, as a whole, compensate for the loss.

quality that is related to their normal function but also affects their susceptibility to disease. Such qualities could be known distinctions such as motor unit size, fiber type, or expression of markers such as trophic factor receptors or transcription factors. Alternatively, there might be unknown distinctions. In either case, these variations could render motor neurons differentially sensitive to SOD1, defects in retrograde transport (LaMonte et al., 2002; Hafezparast et al., 2003), glutamate toxicity (Rothstein et al., 1990) or other proximal causes of pathology. If such differences exist, it should be possible to use expression profiling methods to seek molecular correlates, and eventually mediators, of the relevant distinction. This insight may have important therapeutic potential.

ACKNOWLEDGMENTS

We thank Tim Holy and Ju Lu for assistance with statistical analyses and members of the Lichtman and Sanes labs for helpful discussion.

LITERATURE CITED

Azzouz M, Ralph GS, Storkebaum E, Walmsley LE, Mitrophanous KA, Kingsman SM, Carmeliet P, Mazarakis ND. 2004. VEGF delivery with retrogradely transported lentivector prolongs survival in a mouse ALS model. Nature 429:413–417.

Balice-Gordon RJ, Lichtman JW. 1990. In vivo visualization of the growth of pre- and postsynaptic elements of neuromuscular junctions in the mouse. J Neurosci 10:894–908.

Bradley WG, Good P, Rasool CG, Adelman LS. 1983. Morphometric and biochemical studies of peripheral nerves in amyotrophic lateral sclerosis. Ann Neurol 14:267–277.

Brown RH. 2004. Adult and juvenile amyotrophic lateral sclerosis and related motor neuron diseases. In: Engel AG, Franzini-Armstrong C, editors. Myology. New York: McGraw Hill. p 1865–1888.

Brown WF, Chang KM. 2000. Spinal motor neurons in amyotrophic lateral sclerosis: pathophysiology and motor unit counting. In: Brown RH, Meininger V, Swash M, editors. Amyotrophic lateral sclerosis. London: Martin Dunitz. p 145–160.

Bruijn LI, Becher MW, Lee MK, Anderson KL, Jenkins NA, Copeland NG, Sisodia SS, Rothstein JD, Borchelt DR, Price DL, Cleveland DW. 1997. ALS-linked SOD1 mutant G85R mediates damage to astrocytes and promotes rapidly progressive disease with SOD1-containing inclusions. Neuron 18:327–338.

Bruijn LI, Miller TM, Cleveland DW. 2004. Unraveling the mechanisms involved in motor neuron degeneration in ALS. Annu Rev Neurosci 27:723–749.

Buchthal F, Pinelli P. 1953. Action potentials in muscular atrophy of neurogenic origin. Neurology 3:591–603.

Chiu AY, Zhai P, Dal Canto MC, Peters TM, Kwon YW, Prattis SM, Gurney ME. 1995. Age-dependent penetrance of disease in a transgenic mouse model of familial amyotrophic lateral sclerosis. Mol Cell Neurosci 6:349–362.

Clement AM, Nguyen MD, Roberts EA, Garcia ML, Boillee S, Rule M, McMahon AP, Doucette W, Siwek D, Ferrante RJ, Brown RH Jr, Julien JP, Goldstein LS, Cleveland DW. 2003. Wild-type nonneuronal cells extend survival of SOD1 mutant motor neurons in ALS mice. Science 302:113–117.

Cleveland DW, Rothstein JD. 2001. From Charcot to Lou Gehrig: deciphering selective motor neuron death in ALS. Nat Rev Neurosci 2:806–819.

Dengler R, Konstanzer A, Kuther G, Hesse S, Wolf W, Struppler A. 1990. Amyotrophic lateral sclerosis: macro-EMG and twitch forces of single motor units. Muscle Nerve 13:545–550.

Dyck PJ, Stevens JC, Mulder DW, Espinosa RE. 1975. Frequency of nerve fiber degeneration of peripheral motor and sensory neurons in amyotrophic lateral sclerosis. Morphometry of deep and superficial peroneal nerves. Neurology 25:781–785.

Feng G, Mellor RH, Bernstein M, Keller-Peck C, Nguyen QT, Wallace M, Nerbonne JM, Lichtman JW, Sanes JR. 2000. Imaging neuronal subsets in transgenic mice expressing multiple spectral variants of GFP. Neuron 28:41–51.

Fischer LR, Culver DG, Tennant P, Davis AA, Wang M, Castellano-Sanchez A, Khan J, Polak MA, Glass JD. 2004. Amyotrophic lateral sclerosis is a distal axonopathy: evidence in mice and man. Exp Neurol 185:232–240.

Frank E, Gautvik K, Sommerschild H. 1975. Cholinergic receptors at denervated mammalian motor end-plates. Acta Physiol Scand 95:66–76.

Frey D, Schneider C, Xu L, Borg J, Spooren W, Caroni P. 2000. Early and selective loss of neuromuscular synapse subtypes with low sprouting competence in motoneuron diseases. J Neurosci 20:2534–2542.

Gurney ME, Pu H, Chiu AY, Dal Canto MC, Polchow CY, Alexander DD, Caliendo J, Hentati A, Kwon YW, Deng HX, et al. 1994. Motor neuron degeneration in mice that express a human Cu,Zn superoxide dismutase mutation. Science 264:1772–1775.

Hafezparast M, Klocke R, Ruhrberg C, Marquardt A, Ahmad-Annuar A, Bowen S, Lalli G, Witherden AS, Hummerich H, Nicholson S, Morgan PJ, Oozageer R, Priestley JV, Averill S, King VR, Ball S, Peters J, Toda T, Yamamoto A, Hiraoka Y, Augustin M, Korthaus D, Wattler S, Wabnitz P, Dickneite C, Lampel S, Boehme F, Peraus G, Popp A, Rudelius M, Schlegel J, Fuchs H, Hrabe de Angelis M, Schiavo G, Shima DT, Russ AP, Stumm G, Martin JE, Fisher EM. 2003. Mutations in dynein link motor neuron degeneration to defects in retrograde transport. Science 300:808–812.

Herndon LA, Schmeissner PJ, Dudaronek JM, Brown PA, Listner KM, Sakano Y, Paupard MC, Hall DH, Driscoll M. 2002. Stochastic and genetic factors influence tissue-specific decline in ageing *C. elegans*. Nature 419:808–814.

Kasthuri N, Lichtman JW. 2003. The role of neuronal identity in synaptic competition. Nature 424:426–430.

Kawamura Y, Dyck PJ, Shimono M, Okazaki H, Tateishi J, Doi H. 1981. Morphometric comparison of the vulnerability of peripheral motor and sensory neurons in amyotrophic lateral sclerosis. J Neuropathol Exp Neurol 40:667–675.

Keller-Peck CR, Walsh MK, Gan WB, Feng G, Sanes JR, Lichtman JW. 2001. Asynchronous synapse elimination in neonatal motor units: studies using GFP transgenic mice. Neuron 31:381–394.

LaMonte BH, Wallace KE, Holloway BA, Shelly SS, Ascano J, Tokito M, Van Winkle T, Howland DS, Holzbaur EL. 2002. Disruption of dynein/dynactin inhibits axonal transport in motor neurons causing late-onset progressive degeneration. Neuron 34:715–727.

Love FM, Thompson WJ. 1998. Schwann cells proliferate at rat neuromuscular junctions during development and regeneration. J Neurosci 18: 9376–9385.

McComas AJ, Sica RE, Campbell MJ, Upton AR. 1971. Functional compensation in partially denervated muscles. J Neurol Neurosurg Psychiatry 34:453–460.

Nguyen QT, Sanes JR, Lichtman JW. 2002. Pre-existing pathways promote precise projection patterns. Nat Neurosci 5:861–867.

Ohshima T, Ogawa M, Takeuchi K, Takahashi S, Kulkarni AB, Mikoshiba K. 2002. Cyclin-dependent kinase 5/p35 contributes synergistically with Reelin/Dab1 to the positioning of facial branchiomotor and inferior olive neurons in the developing mouse hindbrain. J Neurosci 22: 4036–4044.

Oosthuyse B, Moons L, Storkebaum E, Beck H, Nuyens D, Brusselmans K, Van Dorpe J, Hellings P, Gorselink M, Heymans S, Theilmeier G, Dewerchin M, Laudenbach V, Vermylen P, Raat H, Acker T, Vleminckx V, Van Den Bosch L, Cashman N, Fujisawa H, Drost MR, Sciot R, Bruyninckx F, Hicklin DJ, Ince C, Gressens P, Lupu F, Plate KH, Robberecht W, Herbert JM, Collen D, Carmeliet P. 2001. Deletion of the hypoxia-response element in the vascular endothelial growth factor promoter causes motor neuron degeneration. Nat Genet 28:131–138.

Reaume AG, Elliott JL, Hoffman EK, Kowall NW, Ferrante RJ, Siwek DF, Wilcox HM, Flood DG, Beal MF, Brown RH Jr, Scott RW, Snider WD. 1996. Motor neurons in Cu/Zn superoxide dismutase-deficient mice develop normally but exhibit enhanced cell death after axonal injury. Nat Genet 13:43–47.

Rich M, Lichtman JW. 1989. Motor nerve terminal loss from degenerating muscle fibers. Neuron 3:677–688.

Ripps ME, Huntley GW, Hof PR, Morrison JH, Gordon JW. 1995. Transgenic mice expressing an altered murine superoxide dismutase gene provide an animal model of amyotrophic lateral sclerosis. Proc Natl Acad Sci U S A 92:689–693.

Rosen DR, Siddique T, Patterson D, Figlewicz DA, Sapp P, Hentati A, Donaldson D, Goto J, O'Regan JP, Deng HX, et al. 1993. Mutations in Cu/Zn superoxide dismutase gene are associated with familial amyotrophic lateral sclerosis. Nature 362:59–62.

Rothstein JD, Tsai G, Kuncl RW, Clawson L, Cornblath DR, Drachman DB, Pestronk A, Stauch BL, Coyle JT. 1990. Abnormal excitatory amino acid metabolism in amyotrophic lateral sclerosis. Ann Neurol 28:18–25.

Schaefer AM, Sanes JR, Lichtman JW. 2002. Synapses and motor units in mouse models of ALS and SMA. In: Proceedings of the Society for Neuroscience, 32nd Annual Meeting. p 189.1.

Walsh MK, Lichtman JW. 2003. In vivo time-lapse imaging of synaptic takeover associated with naturally occurring synapse elimination. Neuron 37:67–73.

Wohlfart G. 1957. Collateral regeneration from residual motor nerve fibers in amyotrophic lateral sclerosis. Neurology 7:124–134.

Wohlfart G. 1958. Collateral regeneration in partially denervated muscles. Neurology 8:175–180.

Wong PC, Pardo CA, Borchelt DR, Lee MK, Copeland NG, Jenkins NA, Sisodia SS, Cleveland DW, Price DL. 1995. An adverse property of a familial ALS-linked SOD1 mutation causes motor neuron disease characterized by vacuolar degeneration of mitochondria. Neuron 14:1105–1116.